Available online at www.sciencedirect.com

SCIENCE DIRECT®

International Journal of Solids and Structures 43 (2006) 642–657

INTERNATIONAL JOURNAL OF SOLIDS and STRUCTURES

www.elsevier.com/locate/ijsolstr

Optimum design of a supercavitating torpedo considering overall size, shape, and structural configuration

Edward Alyanak *, Ramana Grandhi, Ravi Penmetsa

Department of Mechanical and Materials Engineering, Wright State University, Dayton, 3640 Colonel Glenn Hwy., OH 45435, United States

Received 28 September 2004; received in revised form 31 May 2005
Available online 22 July 2005

Abstract

A supercavitating torpedo is a complex high speed undersea weapon that is exposed to extreme operating conditions due to the weapon's speed. To successfully design a torpedo that can survive in this environment, it is necessary to consider the torpedo shell as a critical component. The shell of a supercavitating torpedo must be designed to survive extreme loading conditions (depth pressure and thrust loading), meet frequency constraints, and fit inside the cavity generated by the cavitator. In this research, an algorithm to determine the optimal configuration of the torpedo is presented. This method formulates an optimization problem that determines the general shape of the torpedo in order to satisfy the required performance criteria. Simultaneously, a method to determine the optimal stiffener configuration in the torpedo structure is also presented. A torpedo configuration for a desired speed is obtained and the details of the process are thoroughly discussed.

Keywords: Cavitator; Cavity; Supercavitation; Shape optimization

1. Introduction

A supercavitating torpedo is a complex system that experiences extreme operating conditions. The name "supercavitating torpedo" is derived from the cavity of water vapor that is generated at the nose of the torpedo or cavitator [1] and engulfs the complete structure. This cavity separates the torpedo hull from the water, thereby eliminating much of the viscous drag. This allows tremendous speeds to be achieved that

* Corresponding author. Tel.: +1 937 626 0619; fax: +1 937 775 5147.
E-mail address: ealyanak@cs.wright.edu (E. Alyanak).

[1] The cavitator initiates the super-cavity surrounding the torpedo.

0020-7683/$ - see front matter
doi:10.1016/j.ijsolstr.2005.05.040

are on the order of five to ten times the speed of conventional underwater weapons. The development of this weapon for a submarine commanders arsenal could enable a high-speed quick reaction option or a first strike option in different mission scenarios. In either case, a tactical edge would be gained that is currently not available.

While the theoretical mission scenarios of a supercavitating torpedo provide interesting insight into its use, the engineering challenges in its development are monumental. In this development, there are three main challenges to consider: cavity modeling, torpedo control, and structural survivability. In the research presented, a prototype supercavitating torpedo will be developed based on structural survivability using previously developed cavity modeling techniques (May, 1975).

At this point, it is understood that the forces generated to propel a supercavitating torpedo through the water at high speed are not insignificant. The thrust force and corresponding drag force are on the order of thousands of pounds. Also, as with any underwater device, the ability to handle depth pressure cannot be ignored, even when a cavity is surrounding the vehicle.

There has been recent work done by Alyanak et al. (2005) and Ruzzene (2004) with regards to designing the torpedo structure. In Alyanak's work (2005), the optimal structural configuration was determined for a supercavitating torpedo using both radial and longitudinal stiffeners. The optimal stiffener dimensions were presented along with the optimal number of each kind. However, the overall torpedo dimensions were constant and the model was a simple cylinder with a conical nose. Ruzzene did an extensive analysis of both the static and dynamic buckling stabilities of a cylindrical torpedo shell. The affect of varying the number of ring stiffeners was considered in terms of buckling stability. This is done because of the opposing drag and thrust forces applied to the torpedo structure. In this paper, a supercavitating torpedo design is developed. Neither size nor shape is assumed for the final design. The only assumptions made are that the torpedo is axisymmetric, but not necessarily the simple cylinder that has been used thus far in the literature. The torpedo dimensions are found based on the system performance criteria. Within this paper, a set of performance criteria are given and a torpedo structure is determined using MDO that satisfies these criteria.

To accomplish this task, techniques for modeling two-phase supercavitating flows must be utilized. The properties of the flow, such as cavity shape and corresponding drag, must be known. Many techniques have been developed for modeling the cavity shape, and particularly research into the use of computational fluid dynamics has been done by many researchers such as Kunz et al. (2001). At this conceptual design stage, the time and complexity of the CFD solution is not required for the goals of this research. At the next level, potential flow theory has been utilized to represent cavity dynamics by a significant number of researchers including Kirschner et al. (1995, 2002) and Choi et al. (2005). While these techniques provide very reliable solutions for different shape cavitators or cavity piercing fins, the research in this paper is based on a flat disk cavitator. For this case, many algebraic equations representing supercavitation that are developed from experimental data can be used. These equations have been developed by many researchers over many years and compiled into one document by May (1975). Because these analytical equations are historically well respected, they are utilized in the preliminary design stage to determine a criteria for finding the overall length or size of the torpedo. Furthermore, a method for optimal determination of the torpedo shell shape is presented, allowing the final design to deviate from a simple cylinder. Finally, the methods that were presented by Alyanak et al. (2005) are applied to determine the optimal structural configuration of the design.

2. Modeling of supercavitating flow

Cavitation is described by the cavitation number. The supercavitating phenomenon is characterized by very low cavitation numbers. The cavitation number is a non-dimensional quantity that represents the extent of cavitation. The formulation is given as

$$\sigma = \frac{P - P_{\text{cavity}}}{\frac{1}{2}\rho V^2} \tag{1}$$

as found in May (1975).

In this equation, P represents the pressure outside of the cavity. This is equivalent to the depth pressure. Furthermore, P_{cavity} represents the pressure inside the cavity, ρ is the water density, and V is the torpedo speed. For supercavitation to occur, the cavitation number must approach zero. Thus, P_{cavity} approaches P. Therefore if the torpedo is at a given depth the pressure P is equivalent to the depth pressure $P = \rho gd$. As a result of this the depth pressure must be considered for supercavitating torpedo structural survivability. Even at high dynamic pressures this argument still holds. For example, at a velocity of 120 m/s, P_{cavity} is within 98% of P for a cavitation number of 0.01 and a depth of 600 m.

The flow can be characterized by the torpedo speed V, the cavitation number σ defined in Eq. (1), and the cavitator diameter d. The drag coefficient can be determined for a flat disk cavitator by the relation

$$C_{\text{D}} = 0.815(1 + \sigma) \tag{2}$$

where the drag coefficient is defined by

$$C_{\text{D}} = \frac{D}{\frac{1}{2}\rho V^2 A} \tag{3}$$

where D is the drag force and A is the cavitator area, in this case it is $\frac{\pi}{4}d^2$.

From Eqs. (2) and (3) it is easy to see how the drag on the torpedo can be defined by V, σ, and d.

$$D = \frac{\pi}{8} C_{\text{D}} \rho (Vd)^2 \tag{4}$$

Furthermore, the maximum cavity diameter d_{m} can be defined by σ,

$$d_{\text{m}} = d\left[\frac{C_{\text{D}}}{\sigma - 0.132\sigma^{\frac{8}{7}}}\right]^{\frac{1}{2}} \tag{5}$$

from which the cavity length L_{c} can be determined by Eq. (6).

$$L_{\text{c}} = d_{\text{m}}\left[1.067\sigma^{-0.658} - 0.52\sigma^{0.465}\right] \tag{6}$$

The cavity shape can be determined using Eqs. (5) and (6). This is accomplished by utilizing the Logvinovich principle for stationary cavities as presented by Vasin (2001).

$$\frac{S - S_0}{S_k - S_0} = \frac{t}{t_k}\left(2 - \frac{t}{t_k}\right) \tag{7}$$

where S is the cavity cross-sectional area at time t, S_0 is the initial cavity area, S_k is the maximum cavity area, and t_k is the time taken for the area to grow from S_0 to S_k. These quantities can be defined as

$$S_0 = \frac{\pi}{4}d^2 \tag{8}$$

and

$$S_k = \frac{\pi}{4}d_{\text{m}}^2 \tag{9}$$

Assuming the x-axis runs down the longitudinal axis of the cavity and is zero at the cavitator, then

$$t = \frac{x}{V} \tag{10}$$

and

$$t_k = \frac{L_c}{2V} \tag{11}$$

yielding

$$\frac{t}{t_k} = \frac{2x}{L_c} \tag{12}$$

This allows us to write the cavity radius R_c as a function of distance x from the cavitator as

$$R_c(x) = \left[\frac{1}{4}\left\langle\frac{2x}{L_c}\left(2 - \frac{2x}{L_c}\right)\left(d_m^2 - d^2\right) + d^2\right\rangle\right]^{\frac{1}{2}} \tag{13}$$

Eq. (13) gives a full approximation of the cavity shape when Eqs. (5) and (6) are used to define d_m and L_c, respectively.

3. Torpedo sizing information

In order to develop a structure for a conceptual supercavitating torpedo, it is first necessary to determine the ideal overall dimensions suited to a specific set of performance criteria. The size of the torpedo largely depends on the ability to generate a certain cavity size, which in turn depends on the propulsion system guidelines. The propulsion system can be expected to increase in size and weight as its thrust increases. Therefore, it is important to generate the largest cavity possible, or to maximize the cavity volume, for a given thrust output. This cavity volume maximization is also critical because the complete torpedo structure must fit inside these boundaries.

The optimal torpedo size can be optimized for a desired design speed. The first consideration is that the torpedo should be able to fit in the current torpedo tubes used in submarines. Thus, the overall dimensions should be smaller than the current heavyweight torpedoes (5.8 m long and .54 m in diameter).

The second consideration is that the torpedo must operate inside the most stable portion of the cavity. It is acknowledged that the cavity stability is not stationary or steady-state. For non-ventilated cavities there are different types of cavity closures, such as twin vortices behind the cavity or a re-entrant jet. It is important that the cavity be as stable as possible at the intended operating condition of the torpedo. A re-entrant jet is characterized by the following condition:

$$1 \leqslant Fr \times \sigma \leqslant 3 \tag{14}$$

where

$$Fr = \frac{V}{\sqrt{gd}} \tag{15}$$

and g is the acceleration due to gravity.

Eventhough the supercavitating torpedo will be naturally ventilated by the rocket exhaust or other means and the re-entrant jet closure will not be present, satisfying Eq. (14) will further ensure stability at the desired torpedo velocity.

Finally, it is assumed that the torpedo will be half the length of the cavity. This ensures that the torpedo will be operating in the most stable region of the cavitation bubble and not be affected by the very unstable region in the back half of the cavity.

The optimal torpedo size can be found with this information. It is natural to desire the largest cavity possible with the least amount of work needed to create the cavity. Therefore, the optimally sized torpedo will operate in the largest cavity volume with minimal thrust. For a desired design velocity a large cavity volume with minimal trust is represented mathematically by

$$\min\left\{\frac{D}{D_0}-\beta\frac{VC}{VC_0}\right\} \tag{16}$$

such that

$$1 \leqslant Fr \times \sigma \leqslant 3$$

$$\frac{L_c}{2} < 5.8\ \text{m}$$

$$d_m < .54\ \text{m}$$

where D_0 is nominal drag; VC and VC_0 are cavity volume and nominal cavity volume, respectively; and β is a weight factor.

$$VC = \int_{L_c} \pi\{R_c(x)\}^2\,dx \tag{17}$$

The nominal values are determined using a cavitator diameter of $d = 5$ cm and a cavitation number of $\sigma = 0.01$ along with Eqs. (4) and (17). The weight factor will affect the optimal solution based on the propulsion system parameters.

For a desired design velocity of $V = 120$ m/s, the optimal solutions are presented in Figs. 1–3. The discontinuous nature of the solution is caused by the different constrains becoming active in the optimization problem posed by Eq. (16). In Fig. 1 it can be seen that drag is the least when it is heavily weighted in the multi-objective problem posed in Eq. (16). As the weighting becomes more even and then favors a larger volume the drag increases for a given speed, however the cavity volume increases as a pay off. Thus, the

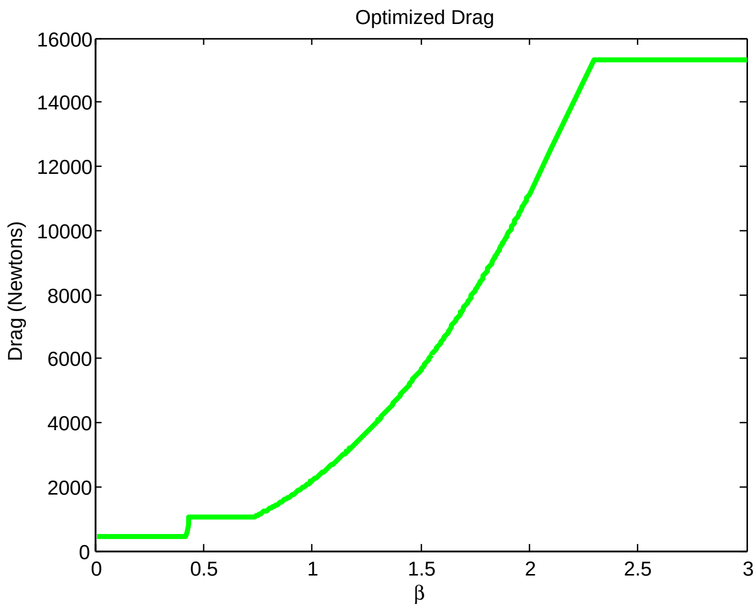

Fig. 1. Optimized drag.

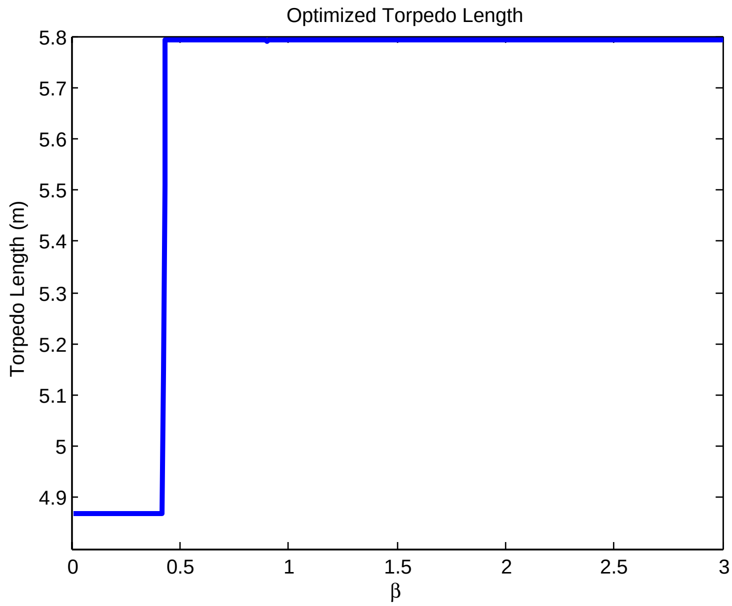

Fig. 2. Optimized torpedo length.

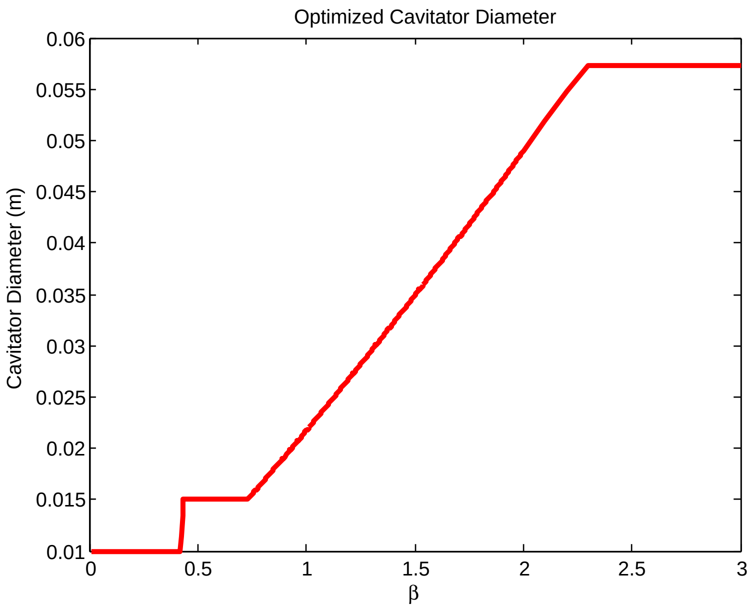

Fig. 3. Optimized cavitator diameter.

drag vs. cavity volume pay off is represented in this figure. In Fig. 2 a similar phenomenon is seen. However, the cavity length is constant and jumps up as problem constraints change to create a longer cavity when cavity volume is considered in the multi-objective problem. In Fig. 3 the optimal cavitator diameter is found

Table 1
Optimal torpedo size and operating conditions

Torpedo size for	$V = 120$ m/s, $T =$ 8000 N
L_{torpedo}	5.8 m
d	0.0415
Operating conditions	
σ	0.0077
L_c	11.6
d_m	0.4433 m

for each weighting possibility given in Eq. (16). It is noted that the diameter increases as volume becomes weighted in the problem. This increase in diameter at the fixed speed of 120 m/s is associated with an increase in drag as shown in Fig. 1 but also increases cavity volume as a pay off.

At this point, the design engineer can determine the optimal solution based on propulsion system specifications. The original intent was to use the specification for an AIM-9 missile solid fuel rocket engine; however, the thrust specifications are classified. Thus, we will assume that a power plant capable of $T = 8000$ N $\sim$ 1800 lbs of thrust T will be used in the torpedo. Then from our optimal solutions, we find the torpedo size specifications and operating conditions given in Table 1.

4. Torpedo design

The structural design and shape of the torpedo based on the gathered information is the focus of this research effort. The performance criteria for the torpedo are given below. The material used will be a titanium–aluminum alloy. It is important to realize that the design criteria affect the final torpedo design and thus can be adjusted as new information becomes available to improve the presented prototype.

1. $\max\{\sigma^{\text{Von Mises}}\} \leqslant 900$ MPa for a depth pressure load equivalent to 600 m depth and a compression load of 8000 N.
2. Thrust buckling factor = 1.25.
3. Collapse buckling factor = 1.25.
4. No natural frequency around 30 Hz.
5. The torpedo body must fit within the bounds of the cavity shape and in the torpedo tube.

The depth of 600 m comes from the maximum operational depth of the Russian nuclear-powered K-141 Kursk submarine. Because operational depth of US NAVY submarines are classified, the Russian version is utilized. Furthermore, the natural frequency in the vicinity of 30 Hz is avoided because the control actuators being examined for supercavitating torpedoes operate close to this frequency. The frequency constraints are estimated with a cantilever boundary condition applied at the cavitator, or torpedo nose. The reason is that the torpedo is only supported at very small locations at the cavitator and possible control fins in the rear, by the surrounding water. Thus, the cantilever boundary condition is a close approximation to the operational natural frequency of the structure. Of course as internal components are created and fit into the torpedo they can be represented as non-structural mass and included in the frequency analysis. The structure is considered empty in the case of this research.

With the criteria stated, it is now desired to develop an optimal torpedo structure that satisfies all of the stated requirements. For research into the optimal design, an objective function was chosen that would not only minimize the structural weight of the torpedo, but would also maximize the internal volume. This is much like the volume maximization required in the previous problem with respect to the cavity size. The reason for structural volume maximization is to include as much space as possible for various torpedo components, such as the propulsion system, guidance system, fuel, warhead, etc. This can be represented mathematically as

$$\min\left\{\frac{m}{m_0}-\Omega\frac{VT}{VT_0}\right\} \tag{18}$$

where m is the torpedo mass, VT is the torpedo volume, and m_0 and VT_0 are the nominal values equal to those of a 4.15 cm cylinder torpedo body with a length of $5.8m$ and a skin thickness of 2.5 mm made of titanium alloy. Therefore, $m_0 = 8.3413$ kg and $VT_0 = 0.0078$ m^3. The weight factor Ω is used to adjust the bias of the multi-objective function towards mass or volume.

5. Finite element modeling

The torpedo models in this research are constructed using finite elements. The use of finite elements allows the analysis of several different design configurations with a minimal cost. The models developed make extensive use of three basic element types. The main element used is a four-node plate element with five degrees of freedom at each node. The second element is the three-node triangle version of the four-node element. Finally, two-node beam elements are utilized to represent the ring and longitudinal stiffeners that are used in some of the models.

A mathematical representation of the expected response of different torpedo designs can be determined with these finite element models. The structural responses of interest are those present in the objective function or constrains of the optimization problem. Thus, mass, stress, natural frequency, and an estimation of buckling stability are required to solve this problem.

Mass is simply determined by summing the product of the volume and density of each finite element over the entire model. Mass will change as the sizing of the structural components varies, as well as when the torpedo body shape changes.

The stresses present in the torpedo model are based on the presence of applied loads. In this case, these loads are depth pressure and thrust force. These loads are contained in the vector $\{f\}$. The structural stiffness of the model is mathematically contained in the stiffness matrix $[K]$. With these two pieces of information, the structural displacements, $\{d\}$, can be found from

$$[K]\{d\} = \{f\} \tag{19}$$

An eigenvalue problem must be solved to determine the natural modes of the structure. In Eq. (20), the free vibration problem is given

$$[K]\{\phi\} = \omega^2[M]\{\phi\} \tag{20}$$

Here, $[K]$ is the same global stiffness matrix of the torpedo model, $[M]$ is the global mass matrix of the torpedo model, $\{\phi\}$ is an orthogonal eigenvector, and ω is the corresponding natural frequency. This information is needed to determine if the frequency constraint is violated by the torpedo design.

Finally, the bifurcation buckling load was considered to determine an estimation of buckling stability. A bifurcation buckling load is the load at which the system may be in equilibrium both in the static sense and also infinitesimally close to being in equilibrium in a buckled configuration. A static reference load is utilized to calculate this load. This is simply a static analysis done with respect to the depth pressure loading condition at 600 m or the thrust loading, as seen in Eq. (19). This is referred to as the reference load $\{f\}_{\text{ref}}$ and the resulting stresses in the elements from this load are contained in $[K_\sigma]_{\text{ref}}$, where $[K_\sigma]$ is the level of stress in the structure known as the geometric matrix. By linear superposition

$$[K_\sigma] = \lambda[K_\sigma]_{\text{ref}} \tag{21}$$

for

$$\{f\} = \lambda\{f\}_{\mathrm{ref}} \tag{22}$$

where λ is simply a scalar multiplier. To determine the load at which the structure buckles, a critical value for λ must be found. This can be determined by solving the arising eigenvalue problem, the formulation of which is given in Eq. (23),

$$([K] + \lambda_{\mathrm{cr}}[K_{\sigma}]_{\mathrm{ref}})\{\phi_{\mathrm{b}}\} = \{0\} \tag{23}$$

In this equation, λ_{cr} is the critical multiplier, and ϕ_{b} is the eigenvector or buckling mode shape. Thus, by finding λ_{cr} we can determine how close the structure is to buckling due to the applied pressure or thrust loads. A value of one or less would imply failure. That is why the constraint is set such that the buckling factor for both loading conditions considered must be greater than 1.25 in magnitude, which results in a safety factor of 25%.

6. Structural configuration

To build the model, it is first necessary to determine the types of configurations that will be analyzed. In the design presented, the torpedo body shape, skin thickness, number of ring stiffeners and longitudinal stiffeners, ring stiffener height and width, along with longitudinal stiffener height and width are the design variables. The orientation of both types of stiffeners are better defined in Fig. 4.

Fig. 4 demonstrates that ring stiffeners will increase resistance to radial loading, such as depth pressure. Conversely, longitudinal stiffeners will increase transverse bending stiffness. The number of stiffeners included, if any, will be determined during the development of the torpedo structure.

As previously stated, it is desired to determine the optimal shape of the torpedo body. Traditionally, the literature has used cylindrical shells for analysis (not even cylindrical torpedo models!). Cylindrical torpedo models will at least include the effects of the nose and tail of the torpedo. Thus, the results are only useful in a St. Venant sense. To achieve this objective, the shape of the torpedo body is defined by five radius values along the length. The radius at the front of the torpedo is equal to the cavitator radius (2.075 cm) determined previously. The other four radius values are defined evenly along the length of the torpedo body, including the aft radius. A cubic spline is fit through these radius points to define the torpedo body shape

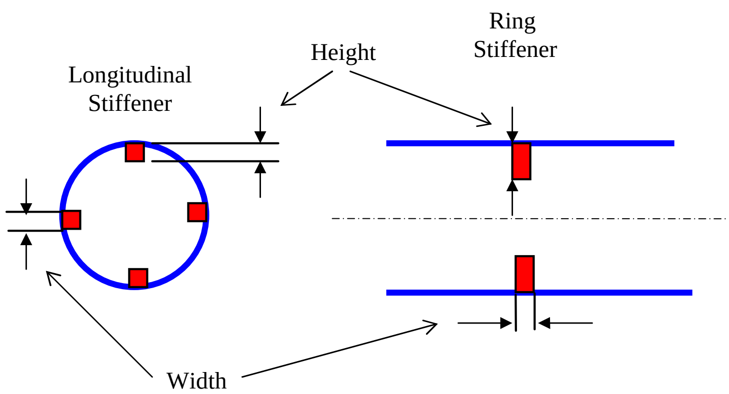

Fig. 4. Stiffener orientation.

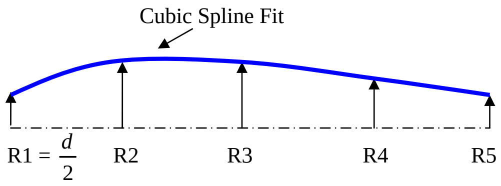

Fig. 5. Torpedo shape definition.

as shown in Fig. 5. From this curve a series of points along the spline can be found to place the nodes that make up the finite element model geometry.

Finally, by employing all the described techniques, a finite element model can be constructed. As stated, the skin is represented with a quadrilateral surface element. There are 60 elements along the length of the torpedo and 16 elements in the radial direction, which yield 960 surface elements defining the torpedo body. The ends of the torpedo are closed with 16 triangular surface elements on each end.

When stiffeners are included in the model, they are represented with beam elements. Each longitudinal stiffener contains 60 beam elements and each ring stiffener contains 16 beam elements. The height and width orientation of these elements is given in Fig. 4.

The thrust force is applied to the aft section of the model by applying point forces at each node in the rear, while the front of the model is constrained. The depth pressure force is applied to the model by applying radial pressure loads. These loads are interpolated into point loads on the nodes with respect to the elemental shape functions. The torpedo model is then constrained from rigid body translation but free to expand and contract due to the applied pressure forces.

The finite element model is created in MATLAB (1997) by selecting the desired values for the variables discussed. The design is then analyzed by using the finite element analysis capabilities of GENESIS (2001). Using the MATLAB code to generate each prototype design greatly increases the ease of analyzing many configurations, thus allowing a better final design to be determined.

7. Results and discussion

The optimal torpedo shape and structural configuration were determined using the mathematical tools to analyze many torpedo configurations. Eq. (18) is multi-objective; therefore, it is likely that the optimal solution will vary for different values of Ω. Because exploring this surface of possible multi-objective optimums known as a pareto surface is very expensive, a reduced-order model was used with no stiffeners. Initially a simplified model made up of 180 elements was used to explore the pareto space defined by Ω in Eq. (18). It was found that variations in Ω from 0.01 to 3.0 had no effect on the solution. For small values of Ω the optimization is mass driven. It happens that the optimal mass is also the largest volume. Obviously for larger values of Ω, we would expect the shape variables to be maximum. This happens to be the optimal solution in both cases. The values for the shape variables are given in Table 2 and Fig. 6 for all cases. The maximum shape variable size is defined as 95% of the cavity size at a given location.

Thirty different configurations of stiffeners were optimized using the refined model with 960 elements with the optimal shape determined from the pareto space. The stiffeners were given dimensions of $1.0\,\text{cm} \times 1.0\,\text{cm}$ so that they would have some effect on the model. The numbers or ring stiffeners tested were 0, 2, 3, 5, 6, 7, 11, 13, 16, and 21. The numbers of longitudinal stiffeners were 0, 4, and 16. When optimizing each case to find the optimal skin thickness, it was found that the optimal solution increased in mass as stiffeners were added. This can be seen in Fig. 7. The interpretation is that the added mass of the stiffeners is more than the decrease in mass from a reduction in skin thickness for the optimal solution. Therefore, the

Table 2
Optimal results with no frequency constraints

Mode #	Hz
1	1.48
2	1.48
3	24.49
4	34.01

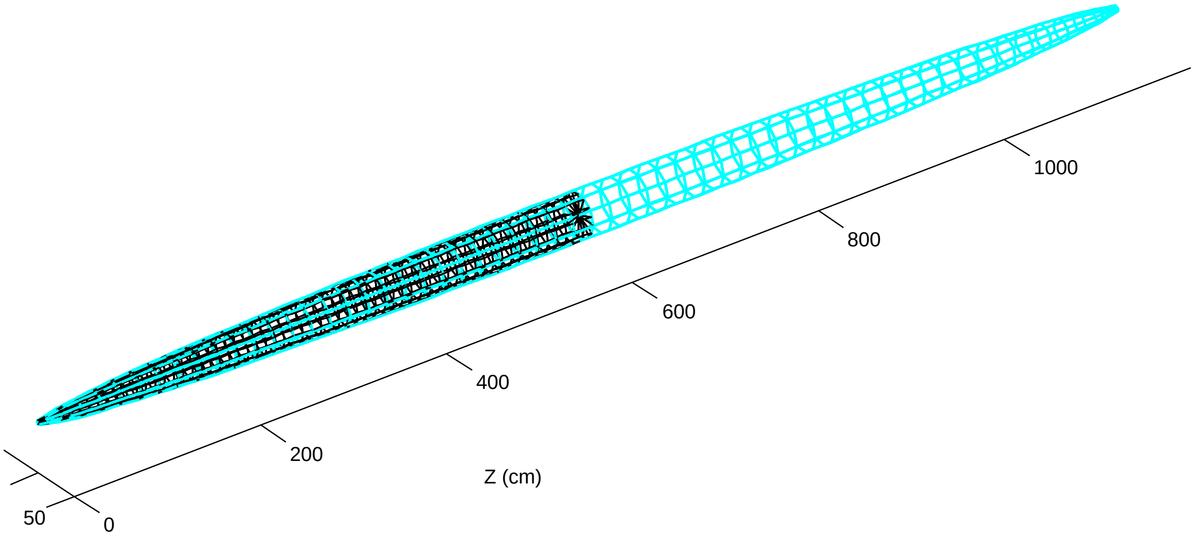

Fig. 6. Optimal torpedo shape in cavity.

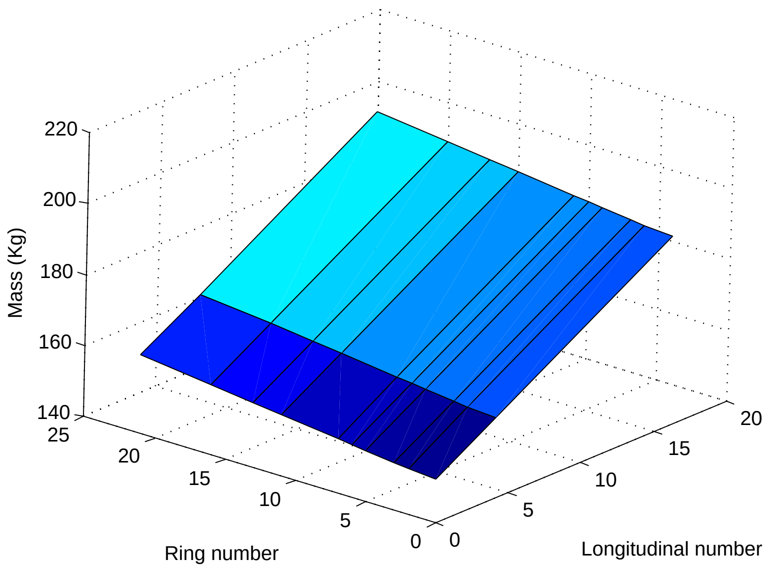

Fig. 7. Stiffener effect on optimized mass objective.

optimal configuration has no stiffeners in the model for constant skin thickness construction and size (1.0 cm × 1.0 cm) stiffeners.

This investigation is not complete because the stiffener size was not considered as a design variable. To truly investigate the optimal structure, it is necessary to disregard potential construction difficulties and cost. This allows the investigation of variable skin thickness as well as allows every potential stiffener in the model to become a design variable. Because the shape is known from our investigation of Eq. (18), the problem has a single objective.

$$\min\{\text{Mass}(\text{stiffener height}, \text{skin thickness})\} \tag{24}$$

subject to stress, frequency and buckling constraints already specified.

The problem posed in Eq. (24) considers each stiffener height as a design variable. The width of each stiffener is set at 0.5 cm to reduce the total number of design variables from 210 to 139. The minimum design value for height is 0.001 cm so that it will be obvious if a stiffener is not required in the model. Furthermore, each ring of surface elements, 60 in total, making up the torpedo body are given a different design variable for thickness, to allow variable skin thickness throughout the design. With these design variables, the developed structural design is general, and efficient use of material is guaranteed.

The frequency constraint posed the most demanding convergence problems. The optimal solution with no frequency constraint placed has natural frequencies near 30 Hz, which indicates a failed design. The optimization results included the frequency values shown in Table 3. The two available solutions were to apply the following options to move the third and fourth modes farther from 30 Hz are:

$$37.5\ \text{Hz} \leqslant \omega_3 \tag{25}$$

or

$$\omega_3 \leqslant 22.5\ \text{Hz} \tag{26}$$

$$37.5\ \text{Hz} \leqslant \omega_4$$

It was found that Eq. (25) caused more difficulties than Eq. (26). This is because the initial values, of various starting points, typically violated the constraint given in Eq. (25) more so than those specified by Eq. (26).

The minimum skin thickness was set to 4.0 mm to avoid unstable pressure buckling problems with lower skin thickness values. At lower skin thicknesses, the stress constraint could be satisfied; however, buckling due to pressure forces became critically low in a highly nonlinear fashion, and the optimizer failed to obtain a feasible solution.

The skin thickness results for the 139 variable problem can be seen in Fig. 8. For the front portion of the model, the skin is at the minimum thickness. However, as the torpedo diameter increases, the skin thickness also increases. Due to the presence of a 1.5 cm end cap at the end, the skin thickness reduces again as the cap is approached. With the inclusion of a given rocket engine and its corresponding dimensions, the end conditions can be modified to fit around the engine and replace the end cap. This will likely change the skin thickness results; however, the solution procedure is unaffected.

Table 3
Optimal shape variables

Shape variable	(cm)
R2	12.73
R3	16.89
R4	20.64
R5	21.06

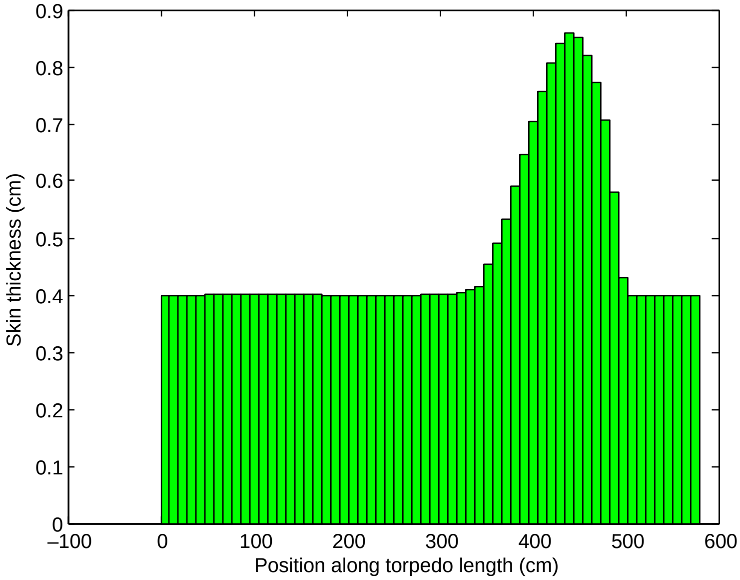

Fig. 8. Skin thickness along torpedo length for 139 variable problem.

The ring height results for the 139 variable problem include 61 rings along the length of the torpedo. These are found in Fig. 9. Again, in the rear of the torpedo the rings respond for the same reason that the skin responds. The maximum stress occurrs at the front of the torpedo. The rings respond to this stress by increasing in height. Also, because the third frequency and fourth frequency are constrained by Eq. (26), the torpedo structure will "manoeuver" to satisfy these conditions. The third frequency is an expansion

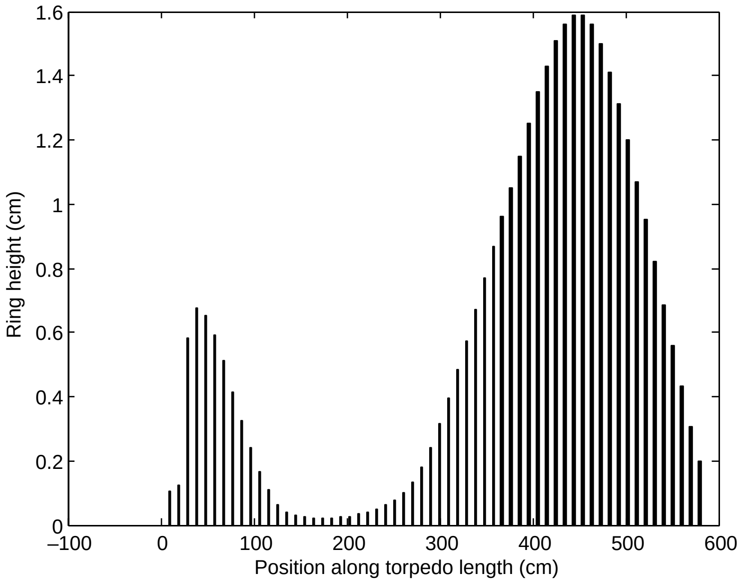

Fig. 9. Ring height for 139 variable problem.

mode, thus increasing the stiffeners will drive this up. This is why the rings tend to disappear in Fig. 9 near the middle of the torpedo. The fourth mode is a bending mode. To increase the frequency this mode which occurs at the torpedo must increase its longitudinal stiffness without increasing the radial stiffness that affects the third frequency, thus satisfying Eq. (26). The optimal place to do this is in the front of the model.

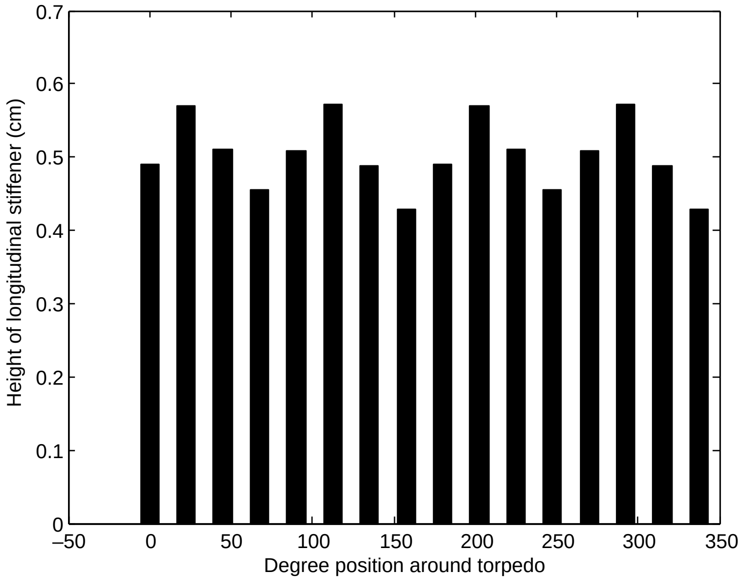

Fig. 10. Longitudinal stiffener height for 139 variable problem.

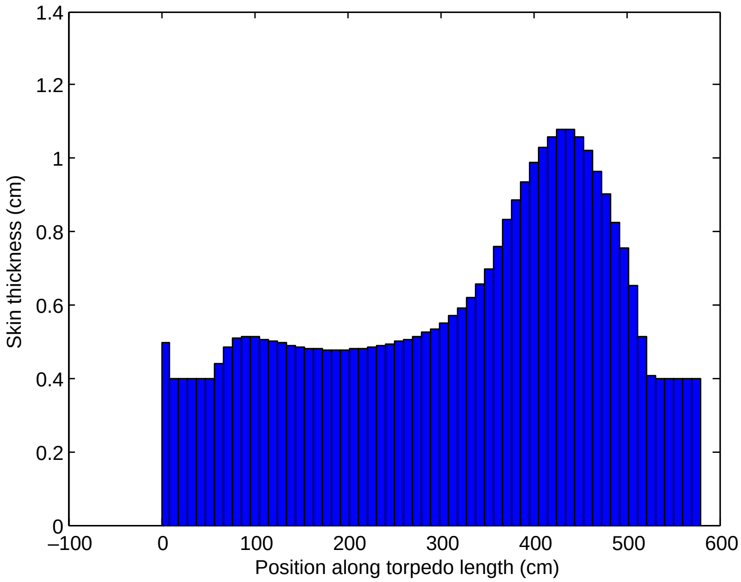

Fig. 11. Skin thickness along torpedo length for reduced problem.

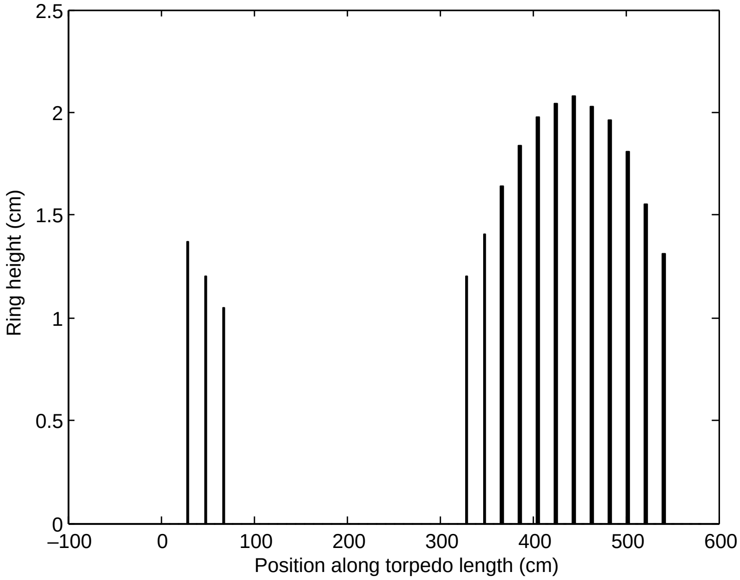

Fig. 12. Ring height for reduced problem.

The longitudinal stiffeners found in Fig. 10 are all under 6 mm in height. Because all 16 are active it is likely that the manufacturing difficulties outweigh the potential gain by including them in the model.

A final problem was run in an effort to have a more manufacturable design. The problem included ring numbers 4, 6, 8, 35, 37, 39, 41, 43, 45, 47, 49, 51, 53, 55, and 57. These rings are in the locations where that maximum response was found from Fig. 9. Also, all 60 design variables for skin thickness were included. Furthermore, the longitudinal stiffeners were taken out of the model. The final results can be seen in Fig. 11 for the skin thickness and Fig. 12 for the reduced ring response.

It is evident that the skin is now taking more load because of the absence of the longitudinal stiffeners. Also, because less rings are included in the front, the skin is also responding to take more load from the reduced number of rings in the front of the model. Also, the skin is responding at the front of the model to tune the frequency constraints and satisfy Eq. (26). The rear of the model responds in the same manner as before. This model, with only 15 rings and no longitudinal stiffeners is significantly less costly to build; however, its main drawback is a weight increase from 163 kg to 184 kg. This increase in 21 kg is significant and represents the penalty for savings cost in manufacturing. At this point the best approach for a supercavitating torpedo prototype will depend on funding and the design team building the structure.

8. Conclusion

A supercavitating torpedo was optimized for overall size, shape, and structural configuration. This was done by taking into account limitations in size that were determined by the torpedo tube size in a submarine. The supercavitating flow was approximated by equations developed and presented in May (1975). These equations are based on experimental evidence and their accuracy is well documented. Using these equations, the optimal torpedo size was found with respect to its length and maximum diameter. By introducing the structural model of the torpedo its optimal shape was found and a simple cylinder shape was no longer used for structural modeling. With the new shape, a high fidelity structural modeling and optimization was carried out to determine the best possible configuration of stiffeners for the torpedo. Because the ‘‘best’’ option would obviously increase manufacturing time and cost, a ‘‘less’’ optimal design was presented and the penalty in torpedo weight was noted.

Acknowledgements

This research work has been sponsored by the office of Naval Research under the Grant. No. 0014-03-1-0057. Dr. Kam Ng is the program manager. We would also like to thank Mr. Aldo Kusmik, NUWC, Newport, RI for providing the direction for this work. Also many thanks to Dr. Vipperla Venkayya and Dr. Ha-Rok Bae for their insight into this problem.

References

Alyanak, E., Grandhi, R., Venkayya, V., Penmetsa, R., 2005. Structural response and optimization of a supercavitating torpedo. Finite Elements in Analysis and Design 41 (6), 563–582.

Choi, J., Penmetsa, R., Grandhi, R., 2005. Shape optimization of the cavitator for a supercavitating torpedo. Structural and Multidisciplinary Optimization 29 (2), 159–167.

GENESIS, 2001. GENESIS User Manual, vol. 1 Version 7.0. Vanderplaats Research and Development, Inc., Colorado Springs, CO 80906, August 2001.

Kirschner, N., Kring, C., Stokes, W., Fine, E., Uhlman, J., 2002. Control strategies for supercavitating vehicles. Journal of Vibration and Control 8, 219–242.

Kirschner, N., Ivan, N., Varghese, A.N., Kuria, I.M., Uhlman, J., 1995. Supercavitating projectiles in axisymmetric subsonic liquid flows. American Society of Mechanical Engineers, Fluids Engineering Division 210, 75–93.

Kunz, R.F., Lindau, J.W., Billet, M.L., Stinebring, D.R., 2001. Multiphase computational fluid dynamics modeling of developed and supercavitating flows. In: Proceedings of VKI Special Course on Supercavitating Flows, von Karman Institute for Fluid Dynamics, Rhode Saint Genese, Belgium, pp. 13-1–13-44.

MATLAB, 1997. Optimization Toolbox Users Guide. The Math Works Inc., Natick, MA.

May, A., 1975. Water Entry and the Cavity-Running Behavior of Missiles. Navsea Hydroballistics Advisory Committee, Arlington, VA.

Ruzzene, M., 2004. Non-axisymmetric buckling of stiffened supercavitating shells: static and dynamic analysis. Computers and Structures 82 (2), 257–269.

Vasin, A.D., 2001. The principle of independence of the cavity sections expansion (Logvinovich’s principle) as the basis for investigation on cavitation flows. RTO AVT Lecture Series on Supercavitating Flows. North Atlantic Treaty Organization, Brussels, Belgium, pp. 8-1–8-27.